Title

Neurocomputational Changes in Inhibitory Control Associated With Prolonged Exposure Therapy

Journal

Journal of Traumatic Stress, 33(4)

ISSN

0894-9867

Authors

Harlé, Katia M
Spadoni, Andrea D
Norman, Sonya B
et al.

Publication Date

2020-08-01

DOI

10.1002/jts.22461

Peer reviewed

Published in final edited form as:
J Trauma Stress. 2020 August ; 33(4): 500–510. doi:10.1002/jts.22461.

Neurocomputational Changes in Inhibitory Control Associated With Prolonged Exposure Therapy

Katia M. Harlé[1,2], **Andrea D. Spadoni**[1,2], **Sonya B. Norman**[1,2], **Alan N. Simmons**[1,2]

[1]VA San Diego Healthcare System, San Diego, California, USA

[2]Department of Psychiatry, University of California San Diego, La Jolla, California, USA

Abstract

Posttraumatic stress disorder (PTSD) is associated with inhibitory control dysfunction that extends beyond difficulties inhibiting trauma-related intrusions. Inhibitory learning has been proposed as a potential mechanism of change underlying the effectiveness of extinction-based therapies such as prolonged exposure (PE), a first-line treatment for PTSD. To identify neurocognitive markers of change in inhibitory learning associated with PE, we applied a Bayesian learning model to the analysis of neuroimaging data collected during an inhibitory control task, both before and after PE treatment. Veterans ($N = 20$) with combat-related PTSD completed a stop-signal task (SST) while undergoing fMRI at time points immediately before and after PE treatment. Participants exhibited a small, significant improvement in performance on the SST, as demonstrated by longer reaction times and improved inhibition accuracy. Amplitude of neural activation associated with a signed prediction error (SPE; i.e., the discrepancy between actual outcome and model-based expectation of needing to stop) in the right caudate decreased from baseline to posttreatment assessment. Change in model-based activation was modulated by performance accuracy, with a decrease in positive SPE activation observed on successful trials, $d = 0.79$, and a reduction in negative SPE activation on error trials, $d = 0.74$. The decrease in SPE-related activation on successful stop trials was correlated with PTSD symptom reduction. These results are consistent with the notion that PE may help broadly strengthen inhibitory learning and the development of more accurate model-based predictions, which may thus facilitate change in cognitions in response to trauma-related cues and help reduce PTSD symptoms.

Prolonged exposure (PE) therapy, an evidence-based manualized psychotherapy based on cognitive behavioral principles, has gained prominence in the treatment of posttraumatic stress disorder (PTSD) and trauma-related psychopathology (Foa, Hembree, & Rothbaum, 2007; Mills et al., 2012). Because it has received significant empirical support that generalizes across different types of trauma, including interpersonal (Foa et al., 2005) and combat-related trauma (Tuerk et al., 2011), PE is recommended as a first-line treatment for PTSD. Grounded on classical conditional principles, the aim of this therapy is to expose patients to the negative, triggering cues at the root of their PTSD symptoms (i.e., reexperiencing, avoidance, and hyperreactivity to those cues and traumatic memories)

Correspondence concerning this article should be addressed to Katia M. Harlé, VA San Diego Healthcare System, 3350 La Jolla Village Drive, San Diego, CA 92161. kharle@ucsd.edu.

in order to facilitate an extinction of the fear response to those cues. The underlying theory is that until those unprocessed trauma-related cues are engaged so that the patient can experience managing the distress associated with the cues, the learned maladaptive responses that create PTSD symptoms will not extinguish and will continue to promote related functional impairment (Foa et al., 2007). Thus, the core focus of PE includes imaginal and in vivo repeated exposure to feared stimuli (e.g., cues and memories), which involve the retelling of the trauma within the safe confines of therapy and approaching specific triggering cues in the patient's real-life environment, respectively (Foa et al., 2007; Foa et al., 2005).

Inhibitory learning, in contrast to fear habituation (Myers & Davis, 2007), is thought to be central to this process of extinction and thus to the effectiveness of exposure-based therapies such as PE (Bouton, 1993; Craske, Treanor, Conway, Zbozinek, & Vervliet, 2014). Within this framework, exposure to the feared conditioned stimulus (CS) without the occurrence of the unconditioned stimulus (US; i.e., the feared event) allows for new learning to occur (i.e., CS occurrence does not mean US is impeding), which overrides initial CS–US associations. Thus, the opportunity to process the co-occurrence of CS and absence of US (i.e., experience expectancy violation) to learn or update the contingency likelihood appears to be a key ingredient of PE therapy. Critically, inhibitory control, and presumably inhibitory learning, which subserves this executive function, appears to be compromised in untreated PTSD, and the degree of this deficit covaries with symptom severity (Aupperle, Melrose, Stein, & Paulus, 2012). Such alterations generally involve impaired performance combined with hyporecruitment of ventrolateral, medial, and inferior prefrontal regions of the brain in the context of proactive control performance (e.g., cognitive reappraisal, inhibitory control tasks; Aupperle et al., 2012). In contrast, successful PE treatment in PTSD has been associated with increased activation of the ventromedial prefrontal fear extinction networks and a concomitant reduced activation of the emotional salience network, particularly the amygdala, in response to feared stimuli (Felmingham et al., 2007). Overall, this research is consistent with the notions that (a) PTSD is associated with inhibitory learning deficits; (b) inhibitory learning is a key ingredient of successful exposure treatment to reduce PTSD symptoms; and (c) extinction-based therapy, such as PE, may facilitate symptom reduction by facilitating learning of new cue–response inhibitory associations (i.e., inhibitory learning). However, thus far, the effect of PE on the neurocognitive processes underlying inhibitory learning has not been specifically investigated. Moreover, it is unclear whether such potential improvement in inhibitory learning is context-specific (i.e., in response to trauma cues) or whether it may provide a more generalized improvement in inhibitory learning.

Computational models, such as error-correction (Rescorla & Wagner, 1972) and Bayesian-based (Yu & Cohen, 2009) learning models, have been recognized as a powerful analytical approach in psychiatric research, as they can help refine the field's understanding of cognitive processing abnormalities in mental illness and identify precise cognitive markers of clinical change and treatment response (Maia, Huys, & Frank, 2017). As such, they can play a pivotal role in advancing theories of the mechanisms of change involved in recovering from psychiatric disorders as well as how various treatments, such as PE, can target those mechanisms (Maia et al., 2017). For instance, a Bayesian learning model (Yu & Cohen,

2009) was recently shown to robustly capture individuals' learned expectations of inhibitory response in the stop-signal task (SST; (Ide, Shenoy, Yu, & Li, 2013; Shenoy & Yu, 2011), a standard inhibitory task in which individuals have to inhibit a learned prepotent motor response (Aron, Fletcher, Bullmore, Sahakian, & Robbins, 2003). This "ideal observer" model assumes that on each trial, individuals track and update their expectation of the stop signal frequency, a dynamic latent belief they in turn use to adjust their action selection speed to minimize error. Using this model, neural markers of inhibitory learning inefficiencies have been identified among substance users of various clinical severity (Harlé et al., 2014; Harlé, Zhang, Ma, Yu, & Paulus, 2016). Specifically, the anterior cingulate and caudate regions of the brain showed abnormal activations to individuals' Bayesian expectations of having to withhold the motor response and to their associated prediction errors, the latter capturing the degree of discrepancy between anticipated and observed cues (i.e., the degree of expectancy violation; Harlé et al., 2014; Harlé et al., 2016). Although the SST probes inhibitory learning in a simple action selection context, this research suggests that a Bayesian learning framework may be relevant and useful for assessing other types of goal-directed inhibitory tasks, such as learning to more accurately anticipate outcomes associated with traumatic cues. Thus, using the SST as an abstraction of inhibitory function and related belief-based adjustment processes may be a reasonable first step to relate potential changes in inhibitory learning to PE effectiveness and symptom reduction and, thus, to determine whether this framework may be relevant to trauma-related learning.

Given the relevance of inhibitory learning to exposure therapy, the goal of the present study was thus to use the formalism of a Bayesian leaning model to assess whether PE does have a systematic impact on inhibitory learning processes and, if so, to identify the neurocognitive markers associated with those treatment-related changes. A second goal of the present study was to investigate whether those potential neurocomputational changes may relate to clinical symptom reduction in individuals with PTSD. We applied a Bayesian learning model to functional magnetic resonance imaging (fMRI) data collected during an SST, both prior to and following a course of PE. As mentioned earlier, providing patients with opportunities to experience expectancy violation to correct their beliefs is one key element thought to promote learning and effectiveness of PE from an inhibitory learning perspective (Craske et al., 2014). Thus, we hypothesized that improved neurocomputational control of motor inhibitory function, reflected by change in neural activation to Bayesian model-based prediction errors during the SST, would be especially related to PE treatment effect and PTSD symptom reduction. We further expected such treatment-related changes to be observed in neural regions such as the anterior cingulate cortex and caudate, which are robustly implicated in tracking prediction errors in the SST and other cognitive interference paradigms (Harlé et al., 2014; Harlé et al., 2016).

Method

Participants and Procedure

The VA San Diego Human Subjects Review Board approved this study protocol, and all participants gave written informed consent. A total of 20 male U.S. military veterans who had been diagnosed with PTSD within the last month and were enrolled in a 12-week

PE treatment for PTSD at the San Diego VA trauma clinic were recruited for the present study; recruited individuals had served in the recent combat operations in Afghanistan and Iraq. Prolonged exposure treatment included psychoeducation about PTSD, exposure in sensu to the traumatic event, and in vivo exposure to avoided activities that functioned as reminders of participants' traumatic experience. Processing of trauma-related emotions and cognitions were encouraged during exposure (see Supplementary Materials). Exclusion criteria included a history of more than 2 years of alcohol dependence, substance abuse in the previous month, use of psychotropic medication within the last 2 weeks (or fluoxetine within the last 6 weeks), lifetime diagnosis of bipolar disorder or schizophrenia, and fMRI-related issues (i.e., irremovable ferromagnetic material, pregnancy, claustrophobia). A diagnosis of comorbid anxiety disorder or major depressive disorder (MDD) was not an exclusion criterion as long as PTSD was the clinically predominant disorder. Participants were included in the present study if they received at least four face-to-face 90-min sessions of PE, which has been shown to be effective in reducing PTSD symptoms (Cigrang et al., 2015). This approach allowed us to assess for any potential dose effect. At both baseline and immediately after completing treatment, participants completed a clinical interview and a functional magnetic resonance imaging (fMRI) session during which they performed various cognitive tasks, including the SST.

Measures

Psychiatric disorders.—Lifetime Axes I and II diagnoses, including PTSD, per criteria from the fourth edition of the *Diagnostic and Statistical Manual of Mental Disorders* (*DSM-IV*), were assessed with the Structured Clinical Interview for *DSM-IV* (SCID; First, Spitzer, Gibbon, & Williams, 1995) and the Clinician-Administered PTSD Scale (CAPS; Blake et al., 1990). These measures have demonstrated high interrater reliability, with a Cohen's kappa coefficient of 0.79 reported for PTSD diagnosis with the CAPS (Aker et al., 1999) and kappa values ranging from 0.50 to 0.98 reported for SCID Axis I disorders (Lobbestael, Leurgans, & Arntz, 2011). Importantly, the concordance rate for diagnosing PTSD between the SCID and CAPS measures is high, $\kappa = 0.89$ (Aker et al., 1999). Verbal intelligence quotient (IQ) and overall intellectual functioning were assessed with the Vocabulary, Matrix Reasoning, and Letter-Number Sequencing modules of the Wechsler Adult Intelligence Scale (WAIS-IV; Wechsler, Coalson, & Raiford, 2008).

Stop-signal task.—To measure potential changes in inhibitory function in relation to PE treatment, participants completed a standard SST while undergoing fMRI, both at baseline (prior to first treatment session) and immediately after completing treatment. In the current study, the SST was composed of 288 trials, 216 (75%) of which were "go" trials and 72 (25%) of which were "stop" trials. Participants were given a standard four-key button-press device with up, down, left, and right options. On go trials, individuals were presented with a go stimulus (an "O" or "X") and tasked with pressing, as quickly as possible, the left button on when an X appeared and the right button when an O appeared. On stop trials, an auditory tone instructing the participant not to press either button was also briefly presented following the appearance of the go stimulus. Each trial lasted until the participant responded up to a maximum 1,300 ms, with a 200 ms interstimulus interval. At both baseline and follow-up, participants also completed the SST before entering the fMRI

scanner to provide practice and establish mean go reaction times (MGRT) from stimuli onset; this allowed us to compute six levels of individually customized stop signal delay (SSD), which provided an equivalent range of difficulty for all participants when performing the task in the scanner. This promoted a mean stop error (SE) rate of 50%. The prescanner task was also administered to ensure that participants where well trained in the task by the time they completed it inside the scanner, to minimize training effects. Participants' MGRT from the prescanner task was used to determine six fixed SSD timings, which they encountered while performing the task in the fMRI scanner. All participants received the same number trials corresponding to each of these six fixed difficulty levels, including "hard" trials, with a longer SSD (i.e., MGRT 0 ms, MGRT 100 ms, MGRT 200 ms) and "easy" trials, with a shorter SSD (MGRT 300 ms, MGRT 400 ms, MGRT 500 ms). The sequence of go and stop trials was pseudorandomized through the task and counterbalanced (for more task details, see Harlé et al., 2014).

Data Analysis

Bayesian model of inhibitory response prediction.—To identify precise neural markers of change in inhibitory function following PE treatment, we applied a Bayes-optimal learning model adapted from the "dynamic belief model" (DBM; Yu & Cohen, 2009). This latent variable model assumes that individuals estimate and update, on a trial-by-trial basis, their belief about the probability of encountering a stop trial based on the observed sequence of trials of the task. This dynamically updated belief is represented by a probability distribution over the unobserved stop signal frequency and the mean of this distribution on each trial, the latent variable "P(stop)." The model further assumes that individuals adjust their behavior (i.e., reaction time [RT]) as a function of this trial-level expectation P(stop). This Bayesian framework of goal-directed behavior has been shown to account for behavioral sequential effects commonly seen in the SST, whereby recently experienced stop trials promote slowing down (i.e., increase RT) on a subsequent go trial in order to minimize the chance of making a commission error. The DBM captures RT adjustments in the SST as well as the race model and its computational form, the drift-diffusion model, which provides a modeling framework for perceptual disambiguation in the SST and other 2-alternative forced-choice tasks. However, DBM-based modeling of the SST has the additional advantage of explaining behavioral changes to contextual manipulation (i.e., fluctuations in true stop signal frequency) and reward or punishment contingencies associated with performance (Ide et al., 2013; Shenoy & Yu, 2011). Importantly, when applied to the SST, this learning model has been successful at predicting individuals' behavior in the task and identifying neural markers of inhibitory function abnormalities that are not otherwise observable behaviorally among clinical and subclinical samples (Harlé et al., 2014; Harlé et al., 2016; Ide et al., 2013). Mathematically, the model assumes that, on each trial, k, the probability of the unobserved stop signal frequency, $p(r_k \mid \mathbf{S}_{k-1})$, is a mixture of the previous posterior distribution, $p(r_{k-1} \mid \mathbf{S}_{k-1})$, and a fixed prior distribution, $p_0(r_k)$, where $\mathbf{S}_k = \{s_1, \ldots, s_k\}$ is the sequence of observed trials up to trial k (i.e., 1 = stop trial, 0 = go trial). The $p(r_{k-1} \mid \mathbf{S}_{k-1})$ and $p_0(r_k)$ probability distributions are weighted by the fixed model parameters α and $1-\alpha$, respectively. On each trial, the probability of trial k being a stop trial, given the sequence of observed trials at this point in the task, $P(s_k = 1 \mid$

$\mathbf{S}_{k-1}$), which, for simplicity, we call P(stop), is the mean of the predictive distribution $p(r_k \mid \mathbf{S}_{k-1})$:

$$p(r_k \mid \mathbf{S}_{k-1}) = \alpha p(r_{k-1} \mid \mathbf{S}_{k-1}) + (1-\alpha)p_0(r_k)$$

The posterior distribution is updated according to Bayes' Rule, being directly proportional to the likelihood of the observed trial outcome multiplied by the prior distribution:

$$p(r_k \mid \mathbf{S}_k) \propto P(s_k \mid r_k)p(r_k \mid \mathbf{S}_{k-1})$$

In the present study, model parameters for the fixed beta distribution $p_0(r_k)$ and α were kept constant across all participants and visits. Indeed, based on simulations with this same paradigm and experimental settings, α and the $p_0(r_k)$ parameter values that maximize model fit at the individual level produced *P*(stop) sequences highly correlated across parameter settings, $r > .90$, $R^2 > .80$, suggesting that a group-level setting is most parsimonious. In addition, using the same parameter settings across participants and visit made any potential observed neural differences associated with P(stop) more readily interpretable. A setting of $Beta(a = 2.50, b = 7.50)$, corresponding to a mean of .25 and a scale of $a + b = 10$, was used for the fixed prior distribution $p_0(r_k)$. This setting was based on previous simulations that sought to maximize the linear fit between true and recovered values for the mean of the fixed prior distribution $p_0(r_k)$ and the α parameter across various settings of the $p_0(r_k)$ scale parameter setting ($s = a + b$). Based on the model assumption of a positive linear association between anticipation of a stop signal and RTs, α was fit to participants' data and inferred based on the setting that maximized the linear regression fit (R^2) of P(stop) on successful go RT across all participants (range tested: .25–1.00, α = .80 maximized overall fit across all participants and visits; Harlé et al., 2014; Ide et al., 2013). Based on these model parameters, individuals' P(stop) sequence was computed and used as parametric regressor in subsequent neural analyses (described later). We note this sequence was the same for everyone given that all participants experienced the same pseudorandomized sequence of go and stop trials. Finally, in order to distinguish inhibitory learning from error learning in the present paradigm, we modeled trial-wise expectations of making an error (P(err)), as the mean of the predictive distribution $p(err_k \mid \mathbf{Z}_k)$, using the same Bayesian learning model, where $Z_k = \{z_1, \ldots, z_k\}$ is the sequence of observed trial outcomes up to trial k (i.e., 1 = error trial, 0 = successful trial). We used fixed parameter settings with a prior distribution consistent with an empirical error rate of roughly half of all stop trials, based on the individual range of SSD targeting a 50% error rate for all participants. Accordingly, we used a parametrization of $Beta(a = 1.25, b = 8.75)$, with a mean = .25 × .50 = .125, which was fit to individuals' sequence of successful and error trials to calculate P(err) on each trial.

Behavioral statistical analyses.—We applied hierarchical generalized mixed-effect linear models to participants' stop trial and RTs (go RT), treating participant as a random factor and other independent variables as fixed effects. The first set of models for go RTs used a linear mixture of P(stop), visit (pre- or posttreatment), number of PE therapy sessions received, and change in CAPS score (i.e., degree of symptom reduction following PE). Go trials with an RT of zero (omission errors) or over 1300 ms were automatically counted as

"go errors," as were wrong key presses, and not included in these analyses. The second set of models for error data used a logit-link function applied to a mixture of P(stop), visit, SSD, number of PE sessions received, and change in CAPS score. We report change in log-likelihood ratio (following a chi-squared distribution) and regression coefficients (when applicable) with associated *t* test and *p* value for any significant effect or interaction.

Image acquisition and preprocessing.—Participants completed each of their scanning sessions (i.e., baseline and posttreatment) on a 3 T General Electric (Boston, MA) scanner with an eight-channel head array coil. On each session, T2*-weighted EPI functional runs, synchronized with the SST stimuli, were collected for each participant (total time about 8:32 min) using an event-related fMRI design with the following parameters: 32 ms echo time, 90° flip angle, 3.43 × 3.43 × 2.60 mm voxels with a 1.40 mm gap, 30 whole brain axial slices, a repetition time (TR) of 2,000 ms, and 256 repetitions. A sagittal high-resolution spoiled gradient recalled anatomical sequence was also acquired at the beginning of each session (25 cm field of view; 256 × 256 matrix; 172 1 mm–thick slices; with 4.8 ms echo time and 8 ms repetition time, 12° flip angle). The SST presentation was projected on a screen visible to participants through a mirror in the head coil. Participants used a standard four-key button-press device to respond to task stimuli.

Preprocessing, normalization to Montreal Neurological Institute (MNI) coordinates, and subsequent fMRI analyses were conducted using ANTsR, a statistical interface between Advanced Normalization Tools Software (ANTs), R statistical software, and Analysis of Functional NeuroImages (AFNI) software (Cox, 1996). Preprocessing steps included removal of temporal outliers, field inhomogeneity correction, slice time correction, and temporal whitening. Motion correction and a CompCor component-based noise correction were also conducted and removed during preprocessing. Outlying acquisitions were censored from the time series using a cutoff rule of 2 standard deviations. Regressors were convolved with a canonical hemodynamic response function (HRF) and entered into a general linear model (GLM) to calculate normalized beta weights and associated statistics. Data were aligned to individual anatomical and MNI template.

First-level fMRI analyses.—Nine task regressors of interest, based on the three main types of trials—go, stop success (SS), and SE—were convolved with a canonical HRF and included as predictors in a first GLM. Go error trials were relatively few (M = 8.50 omissions and M = 1.87 wrong key at baseline; M = 9.83 omissions and M = 2.83 wrong key at posttreatment) and were not included in these analyses (see Supplementary Table 1). Thus, for each trial type, a categorical event-related regressor, a P(stop)-weighted parametric regressor, and a P(err)-modulated parametric regressor were included in this order (Ide et al., 2013), with the parametric regressors being orthogonalized relative to the previous regressor. We included both P(stop) and P(err) modulated regressors in order to distinguish treatment effect on anticipation and learning of the stop response, that is, P(stop), versus anticipation and learning related to accuracy, which could be confounded in regions such as the anterior cingulate cortex (ACC) (Ide et al., 2013). Thus, this first-level GLM provided a way to assess neural activation associated with P(stop) independently of the categorical trial type event and the modulation of P(err) by trial type. To assess for potentially distinct

treatment-related changes in P(stop) model updating processes, we also created a second GLM with the trial-wise Bayesian signed prediction error, that is, SPE; Outcome-P(stop) and unsigned prediction error, that is, UPE; |Outcome-P(stop)|, as parametric regressors of interest. Indeed, whereas SPE can be shown to approximate the degree of Bayesian model updating, thereby capturing the degree of learning (i.e., updating of the Bayesian model–based P(stop) estimate), UPE represents a measure of discrepancy between stop expectations and actual trial type observed in the task. The latter can therefore be understood as an overall tracking index of the P(stop) model goodness-of-fit in contrast to signed trial-level adjustment to P(stop); that is, learning process. This second model also included a regressor modeling trial error (0 = correct or 1 = error) to control for performance error related activity (Ide et al., 2013). Finally, to assess for potential modulation of Bayesian prediction error by trial type, we constructed a third GLM, which was similar to the first one except that for each trial type (go, SS, SE), the second parametric regressor was weighted by a Bayesian SPE instead of P(stop). In addition, the signed prediction error of P(err) (i.e. outcome-P(err)), replaced P(err) for the modulation of the third regressor for each trial type. All GLM models included a baseline regressor that consisted of intertrial intervals with a fixation cross as well as go RTs and SSD as parametric regressors of no interest.

Second-level fMRI analyses.—A voxel-wise linear mixed-effects (LME) model was applied to the regressor *t* statistics of our first-level GLM. Specifically, we tested for the effect of visit (pre- vs. posttreatment) and its interaction with P(stop)-modulated trial type—Go × P(stop), SS × P(stop), or SE × P(stop)—with individual participant treated as random effect. In a first contrast analysis, we isolated P(stop) modulated activations for go versus stop trials (SS and SE were averaged). Whole brain statistical maps were obtained for the visit main effect, reflecting areas tracking P(stop) value irrespective of trial type or accuracy, and the Visit × P(stop)-Modulated trial type interaction. To test potential treatment effect on the modulation of P(stop) activation by overall performance (correct vs. incorrect trials), we conducted a second LME contrast comparing all successful trials (go and SS averaged) to failed trials (SE), obtaining statistical maps for this Visit × P(stop)-Modulated outcome type interaction. Finally, we conducted the same contrast analyses to assess for potential treatment effect on P(err)modulated neural activity, and to distinguish those from any P(stop)-related neural changes. That is, we assessed for the Visit × P(err) weighted trial type (go vs. stop) and the Visit × P(err) weighted trial accuracy (success vs. error) interactions. The *t* statistics and degrees of freedom for each LME contrast of interest were extracted at the voxel level to draw a statistical map of voxel-wise *p* values. To correct for multiple comparisons, we used a cluster threshold adjustment based on Monte Carlo simulations, generated with AFNI's 3dFWHMx and 3dClustSim program (version compiled with AFNI_17.2.17 on September 17, 2017), which computes a three-parameter spatial autocorrelation function applied to participants' detrended preprocessed data to create an optimal smoothing kernel. A minimum of 7 contiguous voxels (i.e., $7 \times 64 = 448$ mm^3) was found to result in a corrected cluster-wise activation probability of $p < .050$ based on a voxel-wise a priori probability of $p < .001$. This method and minimum cluster size have been shown to robustly protect against false positives (Cox, Chen, Glen, Reynolds, & Taylor, 2017; Eklund, Nichols, & Knutsson, 2016).

In subsequent region of interest (ROI) analyses, individual *t* statistics associated with Bayesian prediction error regressors (SPE and UPE) based on the second or third first-level GLM, depending of the significant contrast of interest, were extracted to assess for any treatment-related change in predication error activity. We selectively focused on any area identified in the main effect and interaction contrasts (described earlier) that were consistent with either type of Bayesian prediction errors (UPE and SPE) at the baseline assessment (see Supplemental Materials for rationale). For any cluster of voxels consistent with a significant pre–post change in SPE or UPE activation, we computed the average of the cluster voxels *t* statistics from both baseline and posttreatment. We then computed the change score in such cluster UPE or SPE activation as the difference between those mean *t* scores. This activation change score was then correlated with treatment measures of interest, namely CAPS score and the number of PE sessions received.

Results

Participant Characteristics and Clinical Profiles

Participants were male, an average of 31.95 years of age ($SD = 7.35$), and had completed a mean of 13.81 years ($SD = 1.47$) of education. The sample included 40.0% Caucasian, 30.0% Hispanic, 10.0% African American, and 20.0% Asian American participants. The most common secondary diagnosis, in addition to PTSD, was MDD (65.0%), followed by generalized anxiety disorder (GAD; 20.0%; see Table 1 for participants' demographic and baseline neuropsychological functioning). During treatment, participants completed an average of 10.45 ($SD = 3.95$) individual PE therapy sessions, which took place over an average of 14.71 weeks ($SD = 4.83$). As expected, PTSD symptom severity significantly decreased between baseline (M CAPS score = 89.25, $SD = 15.25$) and posttreatment evaluation (M CAPS score = 54.90, $SD = 29.08$), M score change = −34.35, $t(19) = 6.0$, $p < .001$. Average pre-to-post reductions in scores on CAPS Module B (re-experiencing), Module C (avoidance) and Module D (arousal) were −9.35, −15.30, and 9.70, respectively, ps < .001.

Behavioral Performance and Model-Based Behavioral Adjustment

Consistent with our Bayesian model's assumptions, a positive linear association between go RTs and P(stop) was observed, $B = 238$ ms, $t(19) = 2.8$, $p = .011$; omnibus test: $\chi^2(1, N = 20) = 6.7$, $p = .010$, adjusted $R^2 = .08$. Thus, overall and across visits, participants tended to slow down as P(stop) increased. The main effect of visit on go RT was also statistically significant: $B = 57$ ms, $t(19) = 13.7$, $p < .001$, omnibus test: $\chi^2(1, N = 20) = 184.9$, $p < .001$; M RT at baseline = 687 ms, M RT at follow-up = 738 ms (see Supplementary Figure S1); this pointed to an overall increase in go RT at the posttreatment visit. The P(stop) × Visit interaction was not statistically significant, $\chi^2(1, N = 20) = 0.1$, $p = .832$, which was consistent with similar model fits at both pre- and posttreatment visits. A significant Visit × CAPS Change interaction was also observed, $B = 67$, $t(19) = 8.1$, $p < .001$, omnibus test: $\chi^2(1, N = 20) = 67.2$, $p < .001$; this suggests that individuals with a larger reduction in PTSD symptoms had, on average, longer (i.e., less impulsive) go RTs at their posttreatment assessment. No other significant main effects nor interactions were observed.

As expected in relation to stop trial difficulty, participants had a higher likelihood of error on trials with longer SSD (i.e., closer to their average RT), odds ratio (*OR*) = 1.93, Wald's $z = 22.4$, $p < .001$, omnibus test: $\chi^2(1, N = 20) = 635.0$, $p < .001$ (see Supplementary Figure S1). The visit main effect was also statistically significant, with a significantly lower likelihood of error at the posttreatment assessment, *OR* = 0.30, Wald's $z = -2.1$, $p = .037$, omnibus test: $\chi^2(1, N = 20) = 34.7$, $p < .001$. Moreover, as expected, a negative association between error likelihood and P(stop) was observed, with a smaller likelihood of error as P(stop) increased, *OR* = 0.04, Wald's $z = -2.1$, $p = .040$, omnibus test: $\chi^2(1, N = 20) = 3.9$, $p = .049$. Other main effects (e.g., CAPS change) or interactions (e.g., P(stop) × Visit, P(stop) × SSD, SSD × Visit) did not reach statistical significance, *p*s = .231–.651.

fMRI Analyses

After regressing out any variance correlated with actual stimulus outcome (stop vs. go), we found no areas consistent with an overall visit effect (i.e., pre- to posttreatment change) on P(stop) activation. That is, no neural regions were identified in which the average activation to Bayesian model–based expectations of the "need to stop" (across all trials) changed between baseline and posttreatment assessment. Additionally, no cluster survived correction for multiple comparison for the P(stop)-Weighted Trial Type × Visit interaction contrast. In other words, no neural regions were identified in which the modulation of trial type by model-based expectations of the need to stop significantly changed between baseline and posttreatment assessment.

Modulation of Bayesian prediction of inhibitory response by trial outcome.— Activation of one cluster in the right anterior caudate was associated with a significant interaction between visit and P(stop) weighted trial accuracy (averaged go success and SS vs. SE trials), cluster volume = 10 voxels/640 mm^3; peak voxel coordinates (x, y, z): 19, 23, 10; $F(1, 19) = 26.0$, $p < .001$ (see Figure 1). In this region, negative activations associated with P(stop) were observed on successful go and SS trials at baseline, which significantly decreased, *p*s = .003–.010, and were not different from zero, *p*s = .178–.820, at posttreatment assessment. In contrast, a positive activation to P(stop) on SE trials observed at baseline significantly decreased at posttreatment, $p < .001$, and was no longer different from zero, $p = .090$ (see Figure 2). Based on the fact that P(stop) activation was of similar sign (i.e., negative) on go and SS trials, we specifically extracted SPE activation in this region. Consistent with this P(stop) activation pattern, an observed significant activation to Bayesian SPE on successful trials significantly decreased to a non-zero level at posttreatment, $p < .001$–$p = .004$, $d = 0.97$ for go trials, $d = 0.79$ for SS. In contrast, an SPE deactivation on SE trials at baseline significantly decreased in amplitude at posttreatment, $p = .002$, $d = 0.74$ (see Figure 3A). We note that overall UPE activation at baseline was not significantly different from zero in this region ($M = -0.03$, $p = .861$), which is in contrast to SPE activation ($M = 0.34$, $p = .048$), based on extractions from our second GLM. Moreover, SPE activation decreased at posttreatment to a larger extent than UPE activation, $F(1, 19) = 4.5$, $p = .046$, further pointing to a stronger treatment effect on SPE rather than UPE activation change (see Methods section and Supplementary Materials for rationale).

Further assessing the relation between such pre–post change in P(stop)-based activation and symptom reduction, we found that pre–post change in CAPS score was negatively correlated with pre–post change in P(stop) activation during successful stop trials, *Mdn* voxel-wise correlation coefficient for ROI: $r = -.51$, $p = .022$. Change in CAPS score was also positively correlated with pre–post change in Bayesian SPE activation during successful inhibition, *Mdn* voxel-wise correlation coefficient for ROI: $r = .50$, $p = .025$ (see Figure 3B). In summary, pre- to posttreatment neural changes were consistent with a decrease in positive activation to the signed difference between actual and anticipated need to stop while successfully performing in the task. Importantly, the degree of reduction in this signed difference signal during successful performance was proportional to an individual's reduction in PTSD symptoms.

Modulation of Bayesian prediction of error.—We conducted three similar LME analyses with the P(err) weighted regressors—P(err) × Go, P(err) × SS, P(err) × SE)—to assess for any treatment effect on P(err) modulation by trial type after regressing out any variance correlated with *P*(stop) modulation and trial event alone. Assessed contrasts included (a) Visit × P(err)-Weighted Trial Type (go vs. stop), Visit × P(err)-Weighted Trial Accuracy (success vs. error), and overall visit effect on P(err) activation (independent of trial type). No other regions were identified in those contrast analyses. That is, in contrast to P(stop)-related effects reported earlier, there was no pre–post change in neural activity associated with Bayesian model–based expectation of making an error. This was true regardless of trial type or performance accuracy.

Noncomputational (categorical) regressors.—To ensure that any effect of treatment on P(stop)-modulated activity we observed was significant above and beyond task event–related activation, we conducted three similar LME analyses with the categorical (i.e., non-P(stop)) weighted regressors (go, SS, SE) and their interaction with visit. These analyses did not lead to any significant clusters of activation. We found no regions consistent with either interaction contrast. Thus, the change in P(stop)-related activity reported earlier cannot be accounted for by mere task trial–type effects. This further suggests that the modulation of task events by Bayesian expectations of inhibitory response in the present analyses provides a better model of neural activation change related to PE treatment effects.

Discussion

The goal of the present study was to assess whether a Bayesian framework of inhibitory learning can be useful in assessing the neurocognitive impact of PE on inhibitory control and whether these potential treatment-related changes relate to clinical improvement. Specifically, we wanted to know whether neural activation associated with model-based dynamic expectations of the need to stop (i.e., P(stop)) and associated learning can be modulated by PE and predict PTSD symptom reduction. We specifically assessed for distinct treatment-related effects on two types of Bayesian prediction errors, including one more directly reflecting the amount and direction of model-based P(stop) adjustment (i.e., SPE) and one more generally related to the model goodness-of-fit (i.e., UPE). We found that completing PE (approximately 10 sessions, on average) was associated with a marked decrease in neural activation to P(stop) and related SPE in the right caudate, which was

further moderated by performance accuracy. Specifically, a positive SPE activation on successful trials at baseline was no longer different from zero at posttreatment, and the degree of this decrease on successful stops was correlated with PTSD symptom reduction based on CAPS scores. In contrast, a negative Bayesian SPE activation on SEs at baseline decreased in amplitude at posttreatment assessment, but such change was not related to change in PTSD severity. These neural changes appeared in the context of subtle but significant improvement in behavioral performance, including RT slowing and improved accuracy.

Decreased activation amplitude associated with P(stop) and a Bayesian SPE in the right caudate, in the context of improved behavioral performance, is overall suggestive of a fine-tuning of model-based behavior resulting in better prediction of the need to inhibit. This is reflected by reduced neural signals of signed Bayesian surprise, which reflects the discrepancy between expected and observed outcomes, at posttreatment. This finding is consistent with the notion that PE helps improve inhibitory learning. In the context of exposure to trauma-related cues during such treatment, this improved inhibitory learning may account for the therapeutic effects of PE by adjusting expectations of danger, thus promoting new, more adaptive responses to those cues. Although we did not have a control group, we note (a) the minimum treatment length (at least 4 weeks) and (b) the fact that participants completed an SST of nearly the same length outside the scanner prior to the fMRI task at both pre- and posttreatment assessments. This speaks against a mere training effect occurring between pre- and postassessment and accounting for improved behavioral performance and neural changes.

The caudate is part of an adaptive cognitive processing network with various prefrontal regions, including motor planning areas, such as the presupplementary motor area (SMA) and motor cortex (Duann, Ide, Luo, & Li, 2009) and parietal regions (Di Martino et al., 2008), and it appears to play an important role in cognitive control and learning of stimulus-action associations (O'Doherty et al., 2004). It has also been robustly implicated in coding prediction errors in reward learning and other types of learning-based decision making, such as inhibitory control tasks (Gläscher, Daw, Dayan, & O'Doherty, 2010). Overall, these studies point to a key role of this region in guiding inhibitory performance through learning and an anticipatory model-updating process, which is congruent with the present findings. Moreover, PTSD patients fail to show a decrease in activation to threatening cues in the caudate and other subcortical areas, consistent with a lack of habituation and learning related to threatening cues (Tuescher et al., 2011). Importantly, systematic pre–post decreases in amygdala and caudate activation (particularly right caudate) have been associated with successful cognitive behavioral therapy and PE treatment outcomes in anxious patients (Porto et al., 2009; Whiteside, Abramowitz, & Port, 2012). Overall, this research suggests that treatment-related reductions in caudate activation may be therapeutically beneficial for PTSD patients in cognitive behavioral treatment, which could be related to improved belief adjustment following treatment, as suggested by the present findings.

Although an overall decrease in activation amplitude to such Bayesian prediction errors was observed from pre- to posttreatment across all trial types, it is notable that performance accuracy modulated such activation pattern. Specifically, at baseline, a positive SPE

activation was seen on successful trials, regardless of trial type, whereas a negative SPE activation was observed on error trials. Importantly, this modulation by trial accuracy appears specific to P(stop)-related activation after controlling for activation related to Bayesian model-based P(err) in our analyses. The specific sign of SPE activation on successful versus error trials may reflect the relevance of this prediction signal for motor planning, in terms of, for example, activating a particular motor pathway when performance is successful but inhibiting those or other pathways when an error is made.

The fact that the degree of decreased Bayesian SPE activation on successful trials, and more specifically on successful inhibitory (stop) trials, was correlated with larger reductions in PTSD symptom severity has important clinical implications. That is, participants with larger decreases in SPE activation when successfully inhibiting benefited most from PE treatment. In contrast, although there was also a general pre- to posttreatment decrease in SPE signal on SEs, such reduction was not related to number of PE sessions attended or change in CAPS score. Thus, the ability to fine-tune non–trauma-related inhibitory learning over the course of treatment, as reflected by decreases in expectancy violation neural signals during successful inhibition, may promote improved inhibitory learning associated with trauma, as suggested herein by a reduction in PTSD symptoms. This neural change over the course of treatment, reflected by a larger decrease in SPE activation, may in turn help patients benefit to a larger extent from exposure-based therapies, such as PE. In line with this inhibitory learning framework of exposure, the combination of experiencing discrepancy (i.e., exposure) and learning of new CS–US contingencies appears to be important to the extinction process, or at least to the reduction of maladaptive fear responses, as it promotes new learning and related decrease of expectancy violation (Craske et al., 2014). This is consistent with the modality of PE itself in that patients learn to successfully inhibit unwanted intrusions by exposing themselves to traumatic cues. This, in turn, allows them to experience the discrepancy between their initial heightened expectancies of danger and actual outcome (e.g., absence of dangerous events; Foa et al., 2007). Exposure should then lead to more accurate predictions and decreased discrepancy between expectations and observations during successful inhibition, and, thus, decreased fear-related symptoms. Overall, this finding suggests that individuals with PTSD who show a larger decrease in caudate sensitivity to nonaffective inhibitory learning model updating between start and end of PE treatment may be more likely to benefit from PE and reduce their symptoms.

We note that the present study had several limitations. First, the sample size was small, as there are challenges in enrolling and retaining this veteran population (Mott et al., 2014). As a result, there are still very few clinical studies of this type, which are needed for future research. Based on previous similar computational studies of the SST (Harlé et al., 2014; Ide et al., 2013) and PE pre–post comparisons studies (Powers, Halpern, Ferenschak, Gillihan, & Foa, 2010; Simmons, Norman, Spadoni, & Strigo, 2013), however, large effect sizes were expected (i.e., a Cohen's *d* higher than 0.7) for both symptoms and neural changes, for which our sample size would provide sufficient statistical power. Second, participants in the present study received a range of treatment lengths and intensities in contrast to a fixed manualized treatment length. This, however, increases ecological validity and makes the findings more generalizable to real-world veteran and community populations. Third, the absence of a waitlist or alternative therapy control group makes it difficult to conclude

whether the observed effects are specific to PE versus another modality or to PE versus mere task repetition although we note that participants were substantially habituated to the SST with a prescanning task at both assessment time points. Such controlled studies are needed for future research. Fourth, we note that depression and other comorbidities were prevalent in our sample, as commonly observed in PTSD populations (Rytwinski, Scur, Feeny, & Youngstrom, 2013). Although they are more ecologically valid, the present findings may not generalize to individuals without such comorbidities. Finally, this study was restricted to combat-related PTSD. The present results need to be replicated in a more trauma-relevant inhibitory paradigm and in a broader range of trauma features (e.g., interpersonal).

In conclusion, PE was associated with improved inhibitory learning, as demonstrated by decreased neural expectancy violation signals and improved performance. Moreover, therapeutic effects seem to be specifically linked to the experience of expectancy violation and the selective fine-tuning of model updating activity in the caudate area when successful inhibition occurs. The observation of such neural changes in a relatively small sample and with a general, not trauma-cued, inhibitory control paradigm, further points to a more generalized improvement in inhibitory learning, beyond idiosyncratic trauma narratives. Overall, these findings lend credence to the inhibitory learning model of extinction in the context of PE therapy (Bouton, 1993; Craske et al., 2014). That is, improved inhibitory learning may help facilitate belief adjustment in response to trauma-related cues and expectations, which should reduce anxiety and PTSD symptoms.

Supplementary Material

Refer to Web version on PubMed Central for supplementary material.

Acknowledgments

This research was supported by the Veterans Health Administration (IK2CX001584 to Katia M. Harlé and IK2CX000864 to Andrea D. Spadoni) as well as Merit (I01-CX001542) and Department of Defense Young Investigator grants, awarded to Alan N. Simmons. The authors declare no conflicts of interest.

References

Aker AT, Ozeren M, Basoglu M, Kaptanoglu C, Erol A, & Buran B (1999).Clinician-Administered Posttraumatic Stress Disorder Scale(CAPS) reliability and validity study. Turkish Journal of Psychiatry, 10, 286–293.

Aron AR, Fletcher PC, Bullmore T, Sahakian BJ, & Robbins TW (2003). Stop-signal inhibition disrupted by damage to right inferior frontal gyrus in humans. Nature Neuroscience, 6, 115–116. 10.1038/nn1003 [PubMed: 12536210]

Aupperle RL, Melrose AJ, Stein MB, & Paulus MP (2012). Executive function and PTSD: Disengaging from trauma. Neuropharmacology, 62, 686–694. 10.1016/j.neuropharm.2011.02.008 [PubMed: 21349277]

Blake D, Weathers F, Nagy L, Kaloupek D, Gusman FD, Charney D, & Keane T (1995). The development of a clinician-administered PTSD scale. Journal of Traumatic Stress, 8, 75–90. [PubMed: 7712061]

Bouton ME (1993). Context, time, and memory retrieval in the interference paradigms of Pavlovian learning. Psychological Bulletin, 114, 80. 10.1037//0033-2909.114.1.80 [PubMed: 8346330]

Cigrang JA, Rauch SA, Mintz J, Brundige A, Avila LL, Bryan CJ, . . . Consortium SS (2015). Treatment of active duty military with PTSD in primary care: A follow-up report. Journal of Anxiety Disorders, 36, 110–114. 10.1016/j.janxdis.2015.10.003 [PubMed: 26519833]

Cox RW (1996). AFNI: software for analysis and visualization of functional magnetic resonance neuroimages. Computers and Biomedical Research, 29, 162–173. 10.1006/cbmr.1996.0014 [PubMed: 8812068]

Cox RW, Chen G, Glen DR, Reynolds RC, & Taylor PA (2017). fMRI clustering and false-positive rates. Proceedings of the National Academy of Sciences, 114, E3370–E3371.

Craske MG, Treanor M, Conway CC, Zbozinek T, & Vervliet B (2014). Maximizing exposure therapy: An inhibitory learning approach. Behaviour Research and Therapy, 58, 10–23. 10.1016/j.brat.2014.04.006 [PubMed: 24864005]

Di Martino A, Scheres A, Margulies D, Kelly A, Uddin L, Shehzad Z, … Milham M (2008). Functional connectivity of human striatum: A resting state FMRI study. Cerebral Cortex, 18, 2735–2747. 10.1093/cercor/bhn041 [PubMed: 18400794]

Duann J-R, Ide JS, Luo X, & Li C.-s. R. (2009). Functional connectivity delineates distinct roles of the inferior frontal cortex and presupplementary motor area in stop signal inhibition. Journal of Neuroscience, 29, 10171–10179. 10.1523/JNEUROSCI.1300-09.2009 [PubMed: 19675251]

Felmingham K, Kemp A, Williams L, Das P, Hughes G, Peduto A, & Bryant R (2007). Changes in anterior cingulate and amygdala after cognitive behavior therapy of posttraumatic stress disorder. Psychological Science, 18, 127–129. 10.1111/j.1467-9280.2007.01860.x [PubMed: 17425531]

First MB, Spitzer RL, Gibbon M, & Williams JBW (1995). Structured Clinical Interview for DSM-IV Axis I Disorders. New York, NY: New York State Psychiatric Institute.

Foa EB, Hembree EA, Cahill SP, Rauch SAM, Riggs DS, Feeny NC, & Yadin E (2005). Randomized trial of prolonged exposure for posttraumatic stress disorder with and without cognitive restructuring: Outcome at academic and community clinics. Journal of Consulting and Clinical Psychology, 73, 953. 10.1037/0022-006x.73.5.953 [PubMed: 16287395]

Foa E, Hembree E, & Rothbaum BO (2007). Prolonged exposure therapy for PTSD: Emotional processing of traumatic experiences (treatments that work). New York, NY: Oxford University Press.

Gläscher J, Daw N, Dayan P, & O'Doherty JP (2010). States versus rewards: Dissociable neural prediction error signals underlying model-based and model-free reinforcement learning. Neuron, 66, 585–595. 10.1016/j.neuron.2010.04.016 [PubMed: 20510862]

Harlé KM, Shenoy P, Stewart JL, Tapert SF, Yu AJ, & Paulus MP (2014). Altered neural processing of the need to stop in young adults at risk for stimulant dependence. The Journal of Neuroscience, 34, 4567–4580. 10.1523/jneurosci.2297-13.2014 [PubMed: 24672002]

Harlé KM, Zhang S, Ma N, Yu AJ, & Paulus MP (2016). Reduced neural recruitment for Bayesian adjustment of inhibitory control in methamphetamine dependence. Biological Psychiatry: Cognitive Neuroscience and Neuroimaging, 1, 448–459. 10.1016/j.bpsc.2016.06.008

Ide JS, Shenoy P, Yu AJ, & Li CS (2013). Bayesian prediction and evaluation in the anterior cingulate cortex. Journal of Neuroscience, 33, 2039–2047. 10.1523/JNEUROSCI.2201-12.2013 [PubMed: 23365241]

Lobbestael J, Leurgans M, & Arntz A (2011). Interrater reliability of the Structured Clinical Interview for DSM-IV Axis I disorders (SCID I) and Axis II disorders (SCID II). Clinical Psychology and Psychotherapy, 18, 75–79. 10.1002/cpp.693 [PubMed: 20309842]

Maia TV, Huys QJM, & Frank MJ (2017). Theory-based computational psychiatry. Biological Psychiatry, 82, 382–384. 10.1016/j.biopsych.2017.07.016 [PubMed: 28838466]

Mills KL, Teesson M, Back SE, Brady KT, Baker AL, Hopwood S, … Rosenfeld J(2012).Integrated exposure-based therapy forco-occurring posttraumatic stress disorder and substance dependence: A randomized controlled trial. JAMA, 308, 690–699. 10.1001/jama.2012.9071 [PubMed: 22893166]

Mott JM, Mondragon S, Hundt NE, Beason-Smith M, Grady RH, & Teng EJ (2014). Characteristics of U.S. veterans who begin and complete prolonged exposure and cognitive processing therapy for PTSD. Journal of Traumatic Stress, 27, 265–273. 10.1002/jts.21927 [PubMed: 24948535]

Myers KM, & Davis M (2007). Mechanisms of fear extinction. Molecular Psychiatry, 12, 120. 10.1038/sj.mp.4001939 [PubMed: 17160066]

O'Doherty J, Dayan P, Schultz J, Deichmann R, Friston K, & Dolan RJ (2004). Dissociable roles of ventral and dorsal striatum in instrumental conditioning. Science, 304, 452–454. 10.1126/science.1094285 [PubMed: 15087550]

Porto PR, Oliveira L, Mari J, Volchan E, Figueira I, & Ventura P (2009). Does cognitive behavioral therapy change the brain? A systematic review of neuroimaging in anxiety disorders. Journal of Neuropsychiatry and Clinical Neuroscience, 21, 114–125. 10.1176/appi.neuropsych.21.2.114

Powers MB, Halpern JM, Ferenschak MP, Gillihan SJ, & Foa EB (2010). A meta-analytic review of prolonged exposure for posttraumatic stress disorder. Clinical Psychology Review, 30, 635–641. 10.1016/j.cpr.2010.04.007 [PubMed: 20546985]

Rescorla RA, & Wagner AR (1972). A theory of Pavlovian conditioning: Variations in the effectiveness of reinforcement and nonreinforcement. Classical Conditioning II: Current Research and Theory, 2, 64–99.

Rytwinski NK, Scur MD, Feeny NC, & Youngstrom EA (2013). The co-occurrence of major depressive disorder among individuals with posttraumatic stress disorder: A meta–analysis. Journal of Traumatic Stress, 26, 299–309. 10.1002/jts.21814 [PubMed: 23696449]

Shenoy P, & Yu AJ (2011). Rational decision-making in inhibitory control. Frontiers in Human Neuroscience, 5, 48. 10.3389/fnhum.2011.00048 [PubMed: 21647306]

Simmons AN, Norman SB, Spadoni AD, & Strigo IA (2013). Neurosubstrates of remission following prolonged exposure therapy in veterans with posttraumatic stress disorder. Psychotherapy and Psychosomatics, 82, 382–389. 10.1159/000348867 [PubMed: 24061484]

Tuerk PW, Yoder M, Grubaugh A, Myrick H, Hamner M, & Acierno R (2011). Prolonged exposure therapy for combat-related posttraumatic stress disorder: An examination of treatment effectiveness for veterans of thewars in Afghanistan and Iraq. Journal of Anxiety Disorders, 25,397–403. 10.1016/j.janxdis.2010.11.002 [PubMed: 21131170]

Tuescher O, Protopopescu X, Pan H, Cloitre M, Butler T, Goldstein M, . . . Silverman M (2011). Differential activity of subgenual cingulate and brainstem in panic disorder and PTSD. Journal of Anxiety Disorders, 25, 251–257. 10.1016/j.janxdis.2010.09.010 [PubMed: 21075593]

Wechsler D, Coalson DL, & Raiford SE (2008). WAIS-IV: Wechsler adult intelligence scale. San Antonio, TX: Pearson.

Whiteside SP, Abramowitz JS, & Port JD (2012). Decreased caudate N-acetyl-l-aspartic acid in pediatric obsessive-compulsive disorder and the effects of behavior therapy. Psychiatry Research: Neuroimaging, 202, 53–59. 10.1016/j.pscychresns.2011.11.010 [PubMed: 22704757]

Yu AJ, & Cohen JD (2009). Sequential effects: Superstition or rational behavior. Advances in Neural information Processing Systems, 21, 1873–1880.

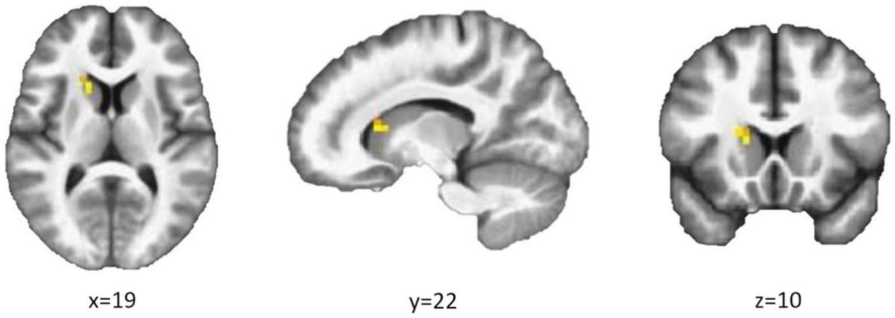

Figure 1.

Blood-oxygen-level-dependent (BOLD) signal associated with a significant interaction between visit (baseline vs. posttreatment) and P(stop)-weighted activation to outcome (success vs. error) in the right caudate, volume = 640 μl; peak voxel (x, y, z): 19, 23, 10; F = 26(1,19), $p < .001$, where P(Stop) is the trial-level expectation of encountering a Stop signal.

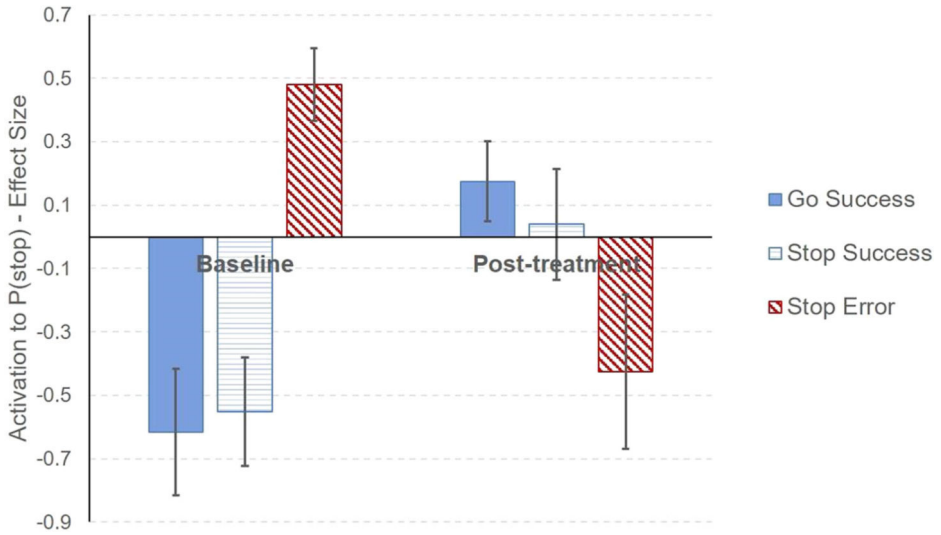

Figure 2.

P(stop) activation by trial type at baseline and posttreatment assessment. Negative activations associated with P(stop) were observed in the right caudate at baseline on successful trials (GO trials and Stop Success/SS trials), which significantly decreased after prolonged exposure (PE) treatment, *p*s = .003–.010, and were not different from zero, *p*s = .178–.820, at posttreatment assessment. In contrast, positive activation to P(stop) on stop error trials at baseline significantly decreased at posttreatment, $p < .001$, and no longer differed from zero, $p = .090$. Error bars indicate standard error of the mean.

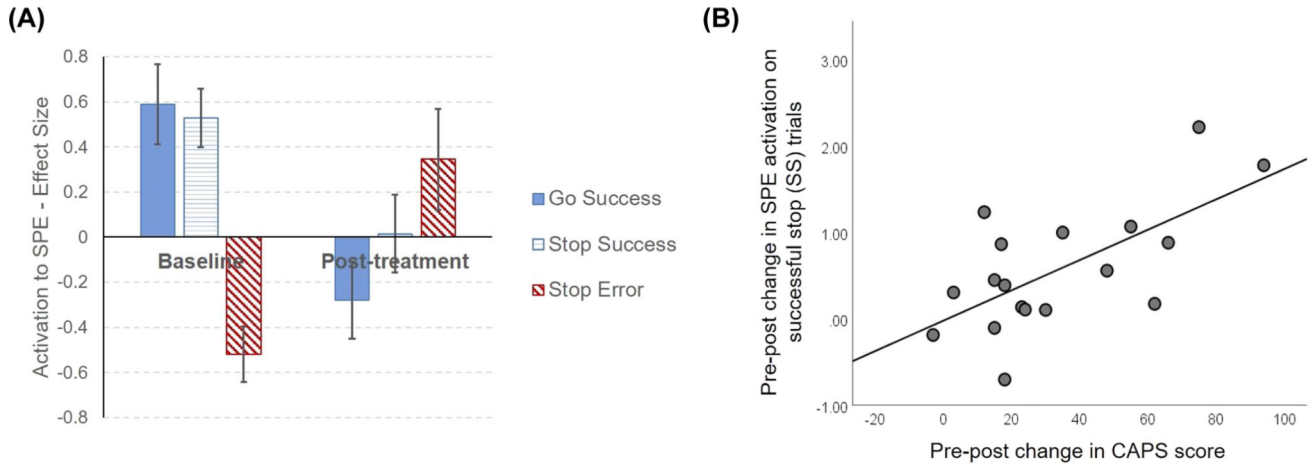

Figure 3.

(A) Activation (*t* statistic) to a Bayesian signed prediction error (SPE) by trial type at baseline and posttreatment assessment. Positive SPE activations were observed in the right caudate at baseline, which significantly decreased after prolonged exposure (PE) treatment, $p < .001$–$p = .004$, and were not different from zero, ps = .135–.930 at posttreatment assessment. In contrast, negative activation to SPE on stop error trials at baseline significantly decreased, $p = .002$, and was no longer different from zero at posttreatment, $p = .110$. Error bars indicate standard error of the mean. (B) Positive correlation between pre–post treatment change in SPE mean caudate cluster activation on successful stop trials and pre–post change in posttraumatic stress disorder (PTSD) symptoms as measured by the Clinician-Administered PTSD Scale (CAPS) total scores. Individuals with larger decreases in SPE activation on successful stop trials had larger decreases in PTSD severity.

Table 1

Demographic and Baseline Neuropsychological Profile

Variable	*M*	*SD*	%	Baseline Assessment *M*	Baseline Assessment *SD*	Posttreatment Assessment *M*	Posttreatment Assessment *SD*
Demographics							
Age (years)	31.95	7.35					
Age at trauma exposure (years)	25.58	6.59					
Time since trauma exposure (years)	5.62	2.99					
Time between trauma exposure and PTSD symptom onset (months)	3.94	11.14					
Education (years)	13.81	1.47					
Race/ethnicity							
Caucasian			40.0				
Hispanic			30.0				
Asian American			15.0				
African American			10.0				
Mixed race/ethnicity			5.0				
Trauma severity scores							
CAPS Total				89.25	15.25	54.90	29.08
CAPS Module B				24.00	5.89	14.65	8.99
CAPS Module C				37.10	7.85	21.80	15.33
CAPS Module D				28.15	4.60	18.45	6.97
Predeployment trauma exposure							
Childhood physical abuse			15.0				
Childhood sexual abuse			5.0				
Neuropsychological functioning scores							
WAIS–Vocabulary[a]				12.05	3.20		
WAIS–Letter-Number Sequencing[a]				9.95	2.95		
WAIS–Letter-Matric Reasoning[a]				11.32	3.27		
Secondary diagnosis							
MDD			65.0				

Variable				Baseline Assessment		Posttreatment Assessment	
	M	*SD*	%	*M*	*SD*	*M*	*SD*
GAD			20.0				
Social phobia			5.0				

Note. PTSD = posttraumatic stress disorder; CAPS = Clinician-Administered PTSD Scale; Module B = reexperiencing symptoms; Module C = avoidance symptoms; Module D = arousal symptoms; WAIS = Wechsler Adult Intelligence Scale; MDD = major depressive disorder; GAD = general anxiety disorder.

[a]Scaled score.